High Power Sunlight-Simulated UV-Induced Radical Polymerization: Self-Initiation and Self-Crosslinking

Author(s):
Yan, Wenqing; de la Vega, Jimena; Eroğlu, Özen; Heisenberg, Lavinia; Wang, Deyi

Publication date:
2024

Permanent link:
https://doi.org/10.3929/ethz-b-000657516

Originally published in:
Macromolecular Materials and Engineering, https://doi.org/10.1002/mame.202300456

Funding acknowledgement:
801781 - Modified Gravity on Trial (EC)

RESEARCH ARTICLE

Macromolecular Materials and Engineering
Open Access
www.mame-journal.de

High Power Sunlight-Simulated UV-Induced Radical Polymerization: Self-Initiation and Self-Crosslinking

Wenqing Yan, Jimena de la Vega, Özen Eroğlu, Lavinia Heisenberg, and Deyi Wang*

Under high power UV irradiation, radicals can be generated from double bonds through photodissociation, H-abstraction, or oxygen initiation mechanisms. This eliminates the need for externally added initiators in photopolymerization. This study investigates high-power sunlight-simulated UV-induced free radical polymerization under various experimental conditions, including the presence of inhibitors, open or closed systems, and partial degassing. Additionally, high-power sunlight-simulated UV-induced atom transfer radical polymerization is explored by externally adding $CuBr_2$/ligand (1:2) catalyst at 100 or 1000 ppm molar concentration of copper. Delicate fabrication of real-world thin films, coatings, and delicate 3D composites further demonstrates the high reliability and versatility of this technology.

1. Introduction

Radical polymerization has been one of the most widely applied techniques in industrial polymer syntheses. It has been developed that subjected to external fields such as temperature, light,[1] electricity,[2] ultrasound,[3] and microwave irradiation.[4] UV-induced radical polymerization is a synthetic technique that utilizes light to initiate and drive polymerization reactions,[5] offering distinct advantages such as rapid reaction rates,[6] spatial and temporal control,[7] sequence-control, and the ability to polymerize a wide range of monomers.[8]

Building upon the concept of simple and green photopolymerization, photopolymerization without a traditional initiator or photoinitiator has emerged as a promising strategy to simplify the polymerization process and avoid inhomogeneous mixing during the use of external initiators. For instance, UV-induced radical polymerization can be initiated by polymer substrate,[9] inorganic system,[10] and dyes.[11]

By utilizing radical polymerization under mechanical forces, Hu et al. explored the mechanochemical synthesis of stimuli-responsive microgels.[12] They successfully synthesized microgels with tailored stimuli-responsive behavior without using any added initiator. This approach provides a novel pathway for designing materials with dynamic properties that can respond to external triggers.

By employing renewable itaconic acid as a monomer, Mielczarek et al. achieved the synthesis of polyampholytes with controlled molecular weights and diverse functionalities. This sustainable approach offers a promising strategy for producing high-performance polymers with precisely controlled properties.[13]

In the realm of controlled radical polymerization, carbon dots were utilized as a green photocatalyst for free radical and atom transfer radical polymerization (ATRP)-based radical photopolymerization under blue LEDs.[14] This innovative approach offers a sustainable and energy-efficient route for initiating polymerization reactions, demonstrating the potential of using carbon dots as environmentally friendly photocatalysts. The ATRP alkyl halide initiator can be formed in situ via photoreduction of $FeBr_3$ by methacrylate monomers.[15]

Under strong UV light, the photoactive monomers themselves can possess the ability to generate radicals or excited states upon exposure to light, initiating the polymerization reaction. The light source serves as the sole initiator for the polymerization process. This mechanism involves the absorption of photons by monomers, leading to the generation of excited states or radicals, which subsequently initiate chain growth. Recent research has explored various aspects of this kind of photopolymerization, demonstrating its broad applicability across different systems and applications. One remarkable application is the self-initiated photopolymerization of anti-inflammatory zwitterionic hydrogels by utilizing a photoactive monomer system, as demonstrated by Stager et al.[16] The resulting zwitterionic hydrogels exhibited excellent biocompatibility and enhanced anti-inflammatory

W. Yan, Ö. Eroğlu
Institute for Building Materials
ETH Zürich, Zürich 8093, Switzerland
E-mail: yanw@ethz.ch
J. de la Vega, D. Wang
IMDEA Materials Institute
C/Eric Kandel 2, Madrid, Getafe E-28906, Spain
L. Heisenberg
Institute for Theoretical Physics
ETH Zürich
Zürich 8093, Switzerland
L. Heisenberg
Institute for Theoretical Physics
Philosophenweg 16, 69120 Heidelberg, Germany

The ORCID identification number(s) for the author(s) of this article can be found under https://doi.org/10.1002/mame.202300456

DOI: 10.1002/mame.202300456

properties, making them promising candidates for sustained drug release in therapeutic applications.

Besides the above-mentioned green initiation strategy, photoinduced radical polymerization has been developed in a way that can be conducted in oxygen-tolerant mild conditions,[17] and effectively using a "green" and inexhaustible sunlight as an energy source for practical low-cost and environmentally friendly curing processes.[18] These collective research endeavors not only advance the knowledge of photopolymerization techniques but also showcase the immense potential of sunlight as an abundant and renewable energy source for polymer synthesis with a broad range of industrial applications.[19]

In this paper, we investigated UV-induced free radical polymerization by using high power sunlight-simulated UV light (HPSS-UV-FRP). Three initiation mechanisms have been proposed. We conducted polymerization reactions using different experimental conditions, such as the presence of inhibitors, utilizing open or closed systems, and implementing partial degassing. The objective was to understand how these parameters affect photopolymerization. Additionally, we explored high power sunlight-simulated UV-induced ATRP (HPSS-UV-ATRP), and studied the reaction mechanisms by adjusting the catalyst concentration and examined the kinetics of the reactions based on monomer conversion. Our target monomers encompassed a wide spectrum, including methacrylates, acrylates, and styrene, offering a robust and diverse set of substrates for examination. Self-crosslinking behavior has been analyzed by estimating the non-dissolved portion of polymers in their good solvent. To demonstrate the applicability of HPSS-UV-FRP in real-world scenarios, we employed this technique to synthesize samples with free polymers, films, coatings, and 3D composites. These applications showcase the reliability and versatility of HPSS-UV-FRP in various practical contexts.

2. Results and Discussion

Traditionally, photopolymerization involves the use of external initiators to generate radicals that initiate the polymerization reaction. However, in our study, we employed two methods for photopolymerization: HPSS-UV-FRP and HPSS-UV-ATRP. These methods were conducted using high power UV light with a sun-simulated spectrum (1000 W m^{-2}).

2.1. Proposed Mechanisms

In the context of our study, we propose three possible mechanisms for HPSS-UV-FRP and HPSS-UV-ATRP, as illustrated in **Scheme 1**. On exposure of methacrylates, acrylates or styrene to UV radiation, active radicals can be generated from the starting monomers. They can be formed through two potential mechanisms: 1) Double bond photodissociation (Scheme 1, Photodissociation), where the C—O and C—C bonds are cleaved, resulting in the generation of radicals.[20] In this case, biradicals can be generated which could lead to crosslinking during the polymerization; 2) Excitation of the double bond to a triplet state (Scheme 1, H-abstraction), enabling hydrogen abstraction and the formation of radicals.[21] These radicals then undergo either free radical polymerization or atom transfer radical polymerization. While oxygen can also be involved in initiation process (Scheme 1, Oxygen initiation), a triplet diradical intermediate can be generated from solvated oxygen reacting with an alkyl acrylate monomer.[22]

In HPSS-UV-ATRP, the formation of activators can happen through two mechanisms (Scheme 1): 1) Addition reaction between monomers and $CuBr_2$, which allows a halogen-exchange mechanism;[23] 2) UV reduction of added $CuBr_2$.[17b]

2.2. HPSS-UV-FRP

We performed first HPSS-UV-FRP at ambient conditions, and investigated how the reaction parameters affect the polymerization, these parameters include the presence of inhibitors, in open or closed systems, and partial degassing (**Figure 1a** and Figure S1). The HPSS-UV-FRP of MMA was observed with M_n 51.7 kDa and $Đ = 1.5$ (Figure 1b). When the polymers at the top of the reaction container (close to the air) are compared with the polymers near the bottom (far from the air), comparable molecular weight values and polydispersity indexes were observed (Figure 1c). This may be because the diffusion of dissolved oxygen molecules and generation of radicals are faster than polymerization, which eliminates the difference of reaction mixtures between the polymer chains generated in two positions. Reaction volume and strength of stirring also affect the results.

We postulated that the dissolved oxygen still plays a role in HPSS-UV-FRP. It has been reported that in the presence of a very small amount of molecular oxygen and in the absence of any thermal initiators, free-radical polymerization of acrylate monomer occurs sustainably and proceeds to a very high monomer conversion.[22] In high power UV-induced polymerization, oxygen can also contribute to polymer chain initiation (mechanism 3 in Scheme 1). However, the participation of oxygen in polymerization may inhibit initiation,[24] when the amount of dissolved oxygen was reduced, less chain termination can happen, leading to shorter chains in open air system. This is in good agreement with SEC data in the experiment of partially degassed reaction mixture (Figure 1d), where polymers with higher molecular weight (≈72 kDa) were obtained, albeit with poor control over the molecular weight distribution ($Đ$ = 1.72). This could be due to the reason that the dissolved nitrogen molecule in the mixture on top was exchanging with oxygen in air, inhomogeneous distribution of dissolved oxygen accounts for high polydispersity index.

This hypothesis is further supported by SEC data when the reaction is conducted in open system (Figure 1e), where more gaseous oxygen is continuously dissolved and get involved in polymerization. Much shorter chains (≈17 kDa) were obtained due to more chain terminations compared to closed system and partially degassed system.

For example, monomethyl ether hydroquinone as inhibitor for methyl methacrylate (MMA), it inhibits the growth of polymer chains by reacting with free radicals. This makes the polymerization process slower and can be used to control the polymerization rate. Although inhibitors can adjust the polymerization rate, in some cases, the control precision may not be as high as ATRP, which can provide more precise molecular weight control and monomer concentration. The extremely low dispersion at the molecular level gives it an advantage in accurately synthesizing polymers with uniform molecular weight. As depicted in Figure 1f, When inhibitors were removed

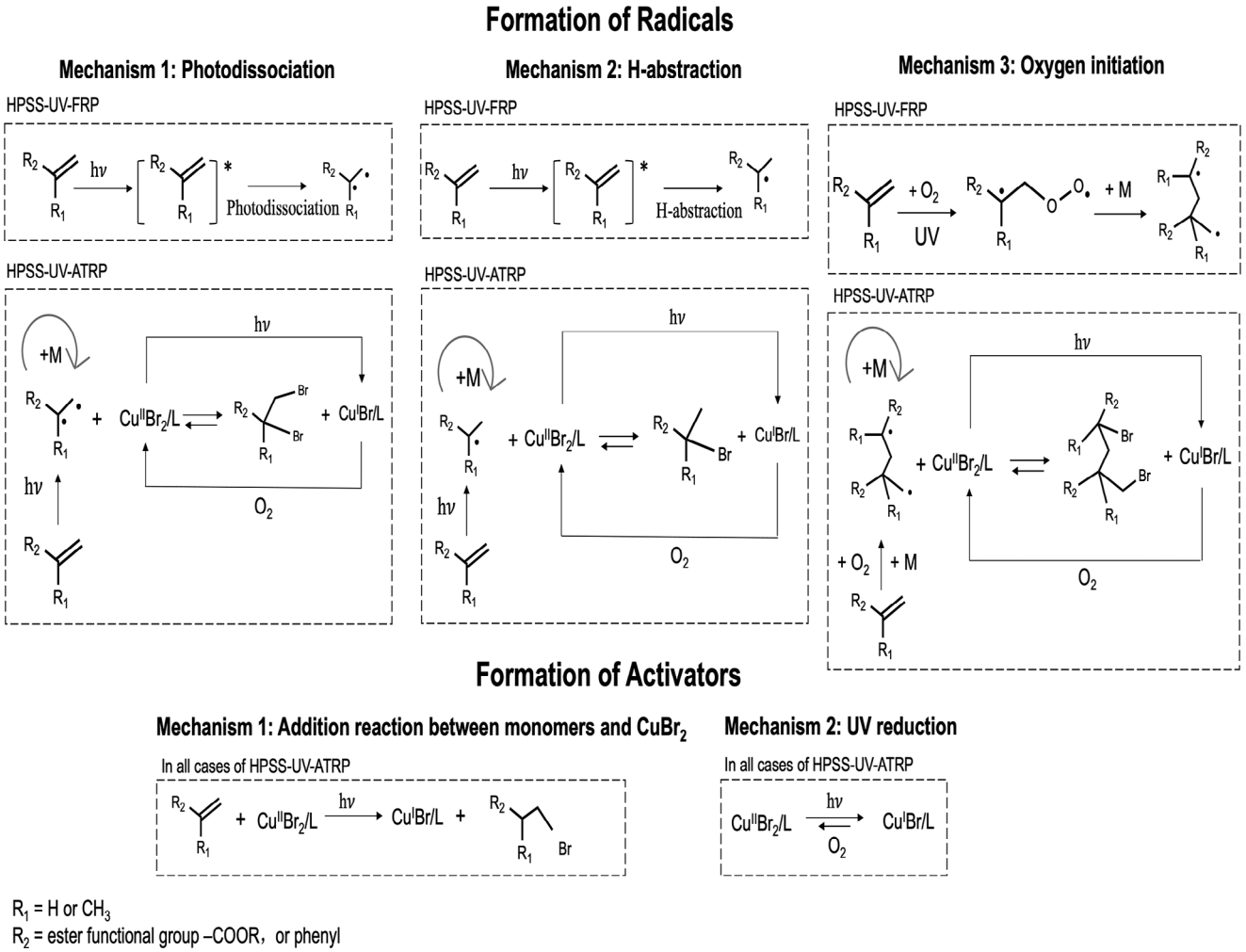

Scheme 1. Proposed possible mechanisms of HPSS-UV-FRP and HPSS-UV-ATRP.

by basic alumina chromatography, high activity of monomers reveals fast propagations and simultaneously a bit more frequent terminations of chains, resulting in lower molecular weight (≈33 kDa), compared to the polymerization with inhibitors (≈51 kDa).

With external addition of initiators (Figure 1g), polymerizations were initiated by both initiator and monomers, resulting in lower molecular weight (≈30 kDa) than expected (≈50 kDa, estimated according to monomer/initiator ratio).

Notably, during analysis, we observed that some polymer did not completely dissolve in good solvent. This incomplete dissolution can be attributed to the formation of crosslinks during polymerization, which occur when radicals generated by photodissociation participate in propagation (Scheme 1) and result in chains containing two radicals. These crosslinks restrict the solubility of the polymer and hinder its ability to fully dissolve in the solvent.

2.3. HPSS-UV-ATRP

HPSS-UV-FRP enables the formation of a polymer by addition of building blocks. In the presence of catalyst, "living" chain ends and high molecular weight can be obtained by controlled radical polymerization. HPSS-UV-ATRP was performed with two different concentrations of $CuBr_2$ catalysts (**Figure 2a**).

We observed a strong crosslinking occurring when we add 1000 ppm ATRP catalyst, which was confirmed by insolubility of polymers in good solvent (Figure 2b). Crosslinking occurred with 1000 ppm instead of 100 ppm [$CuBr_2$]/[Me_6TREN]. One possible reason could be that the polymerization rate was slowed down with an increasing amount of ATRP catalyst, which can be confirmed by ^{1}H-NMR spectrum (**Figure 3**), more initiating radical chains could be generated that increase the concentration of diradicals via photodissociation and oxygen initiation process. Moreover, it is hard to demonstrate the "control" of ATRP in the presence of crosslinked chains.

2.4. Monomer Conversions

Monomer conversion of styrene has been determined by conversion = $(1 - I_{H_b}/I_{H_c}) \times 100\%$ where I_{H_b} is the integral of styrene protons at either 5.1 or 5.6 ppm and I_{H_c} is the integral

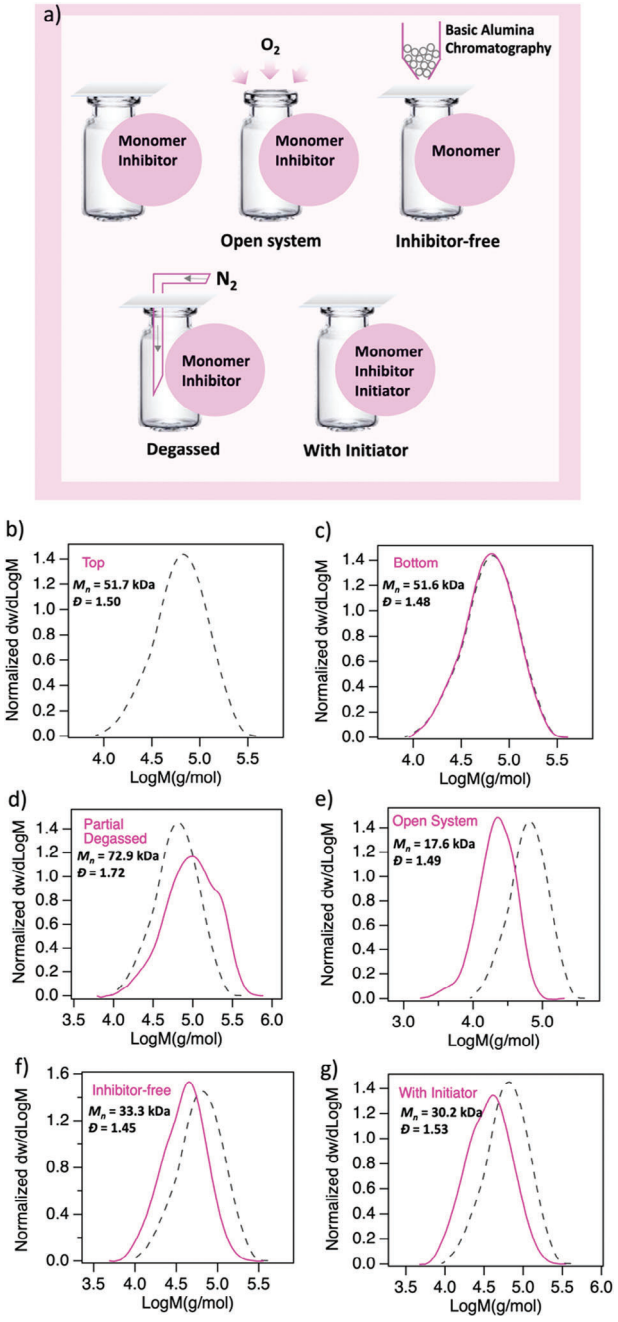

Figure 1. a) Schematic representation of HPSS-UV-FRP of methyl methacrylate with different reactants in different reaction conditions. b) SEC data of HPSS-UV-FRP in closed system, taken from top part where there is air space between reaction mixture and mold. SEC data comparing (b) in different conditions and reactants: c) Samples from the bottom of the mold, where there is no air space between reaction mixture and mold. d) Degassed system, where the monomer mixture was degassed by N_2 purging before polymerization. e) Open system without any cover. f) Inhibitor-free system, where inhibitor in monomer was removed by basic alumina chromatography. g) Reaction mixture with initiator added externally. Reactions were run at ambient temperature for 18 h in a UV chamber (≈1000 W m^{-2}, sunlight-simulated spectrum), with a reaction volume in each case of 2 mL. Black dash line: GPC curve in (a) as a comparison.

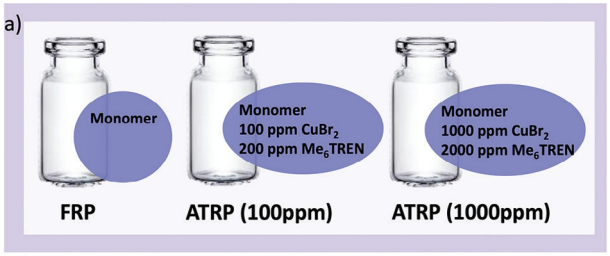

b)

	PMMA		PS	
	Mn (kDa)	PDI	Mn (kDa)	PDI
HPSS-UV-FRP_3h	193.325	1.58	90.511	1.53
HPSS-UV-ATRP-100ppm_3h	115.051	1.52	70.892	1.68
HPSS-UV-ATRP-1000ppm_3h	No signal	No signal	Low signal 186.785	Low signal 1.29
HPSS-UV-FRP_18h	125.053	1.61	96.303	1.53
HPSS-UV-ATRP-100ppm_18h	60.127	1.22	99.677	1.68
HPSS-UV-ATRP-1000ppm_18h	No signal	No signal	No signal	No signal

Figure 2. a) Schematic representation of HPSS-UV-ATRP of styrene, HPSS-UV-ATRP of styrene with 100 ppm catalyst and 1000 ppm catalyst. b) Table: SEC data of HPSS-UV-FRP and HPSS-UV-ATRP of MMA and styrene. 100 ppm $CuBr_2$ or 1000 ppm $CuBr_2$ was added in HPSS-UV-ATRP. The ratio of [$CuBr_2$] to [Me_6TREN] was maintained at 1:2. Reactions were run at ambient temperature for 3 and 18 h in a UV chamber (≈1000 W m^{-2}, sunlight-simulated spectrum), with a reaction volume in each case of 2 mL.

of the protons of polystyrene at 1.94 ppm. The HPSS-UV-FRP of MMA was observed with more than 96% monomer conversion (Figure 3a). In order to check the polymerization kinetics of HPSS-UV-FRP and HPSS-UV-ATRP, we plotted the typical kinetic profile based on ^{1}H-NMR data at different polymerization times (Figure 3b). When comparing HPSS-UV-FRP to HPSS-UV-ATRP, it was observed that the latter presented a lower polymerization rate. Moreover, the polymerization rate was further decreased by increasing the catalyst concentration, as shown in Figure 3d,e and Figure S2–S4. The addition of 100 ppm of $CuBr_2$ led to an increased activity of chain ends. Furthermore, increasing the $CuBr_2$ concentration to 1000 ppm further enhanced the level of control in the polymerization process.

To examine the polymerization kinetics of HPSS-UV-FRP and HPSS-UV-ATRP, we generated a typical kinetic profile using ^{1}H-NMR data collected at various polymerization times (Figure 3b). The HPSS-UV-FRP of MMA demonstrated a monomer conversion of over 96% (Figure 3a). In comparison to HPSS-UV-FRP, HPSS-UV-ATRP exhibited a lower polymerization rate, which was further reduced by increasing the catalyst concentration (Figure 3d,e). This indicates that the addition of 100 ppm of $CuBr_2$ resulted in better control within the system, and the level of control was further enhanced by using 1000 ppm of $CuBr_2$.

HPSS-UV-FRP is a method that allows for the efficient and energy-saving polymerization of a variety of monomers, as listed in **Table 1**. This method provides an opportunity to carry out polymerization processes using environmentally friendly energy sources. No GPC signal was obtained for PMBAA, PDMAEMA, PGMA, PBA, and POEGMA. The reason could be due to strong crosslinking of polymers, which was measured as non-dissolved portion.

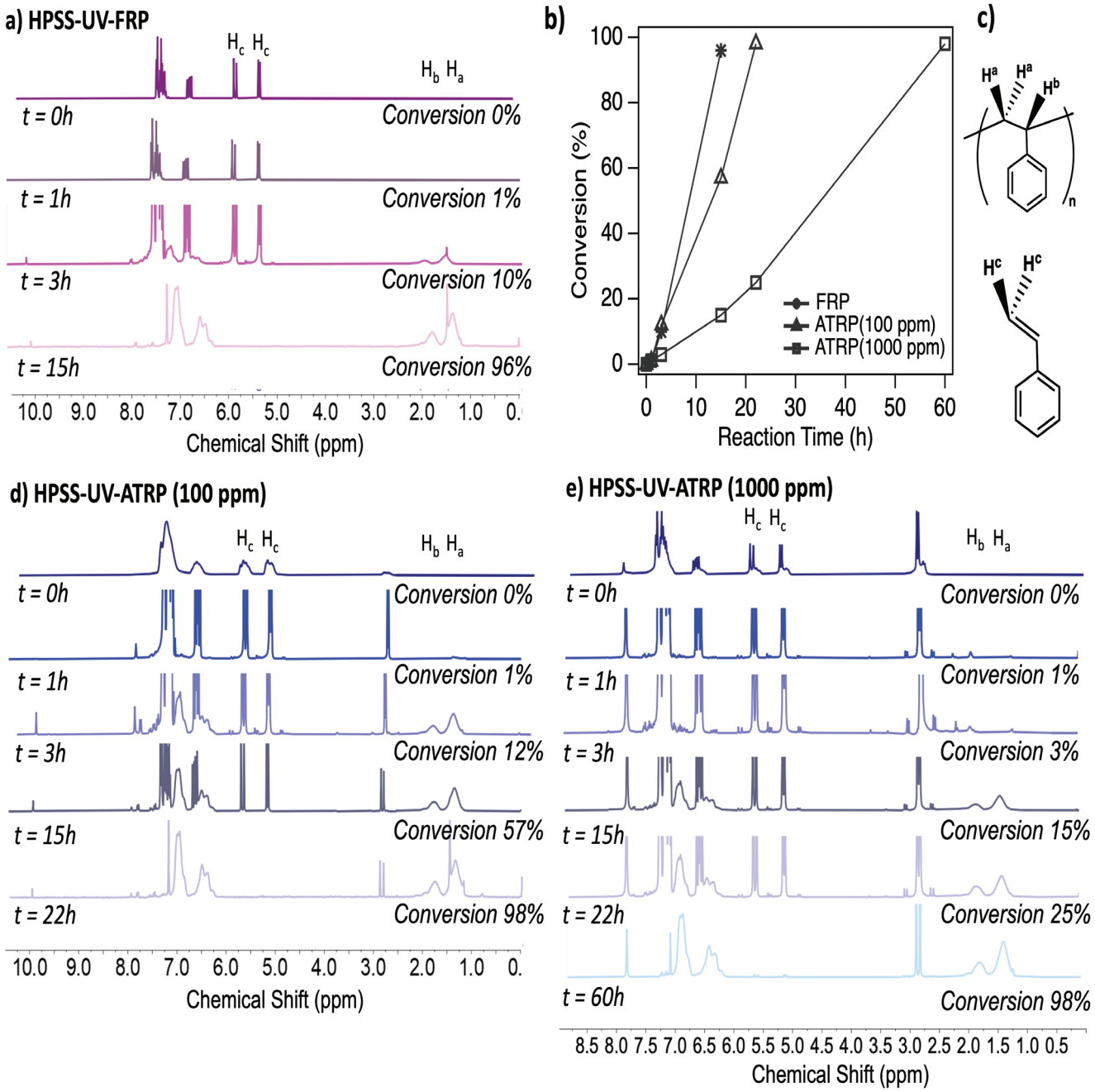

Figure 3. ^{1}H-NMR spectra for increasing reaction times during the synthesis of a) HPSS-UV-FRP. b) Kinetic data comparing HPSS-UV-FRP and HPSS-UV-ATRP. c) Protons in styrene and polystyrene for quantitative analysis of monomer conversions. d) HPSS-UV-ATRP (100 ppm). e) HPSS-UV-ATRP (1000 ppm). Reactions were run at ambient temperature for different polymerization times in a UV chamber (≈1000 W m^{-2}, sunlight-simulated spectrum), with a reaction volume in each case of 2 mL.

2.5. Films and 3D Projects

Figure 4a illustrates the synthesis of thin films with a thickness of ≈80 µm through HPSS-UV-FRP of solely ethylene glycol dimethacrylate (EGDMA). The resulting films exhibit a compact morphology at both the micro- and nanoscale. Furthermore, hydrophobic and hydrophilic coatings were developed on wood by copolymerizing OEGMA/EGDMA and tert-butyl acrylate (tBuA)/EGDMA. 3D objects resembling a tire and a house were fabricated using HPSS-UV-FRP involving styrene and EGDMA. For the synthesis of a bird-shaped polymer network, we introduced a catalyst consisting of 100 ppm $CuBr_2$/Ligand via ATRP. As depicted in Table 1, crosslinking was observed during the polymerization of certain monomers. Hence, we synthesized more intricately crosslinked 3D objects in the absence of additional crosslinkers, as illustrated in Figure 4d. This achievement

Table 1. Monomer conversion in HPSS-UV-FRP measured by ^{1}H-NMR with different monomers with quantified dissolved polymer in their respective good solvent. Reactions were run at ambient temperature for 48 h in a UV chamber (≈1000 W m^{-2}, sunlight-simulated spectrum), with a reaction volume in each case of 2 mL. Non-dissolved portion was calculated by weighing the non-dissolved portion of polymer in their respective good solvent, water for PAA and PNIPAM, THF for the others.

	Monomer conversion	Non-dissolved portion
N,*N*′-methylenebisacrylamide (MBAA)	93%	>99.99 wt%
2-(Dimethylamino)ethyl methacrylate (DMAEMA)	98.5%	>99.99 wt%
Acrylic acid (AA)	97%	91.6 wt%
Glycidyl methacrylate (GMA)	94%	>99.99 wt%
Butyl acrylate (BA)	88%	>99.99 wt%
N-isopropylacrylamid (NIPAM)	85%	56.89 wt%
Oligo(ethylene glycol) methyl ether methacrylate (OEGMA)	98%	>99.99 wt%

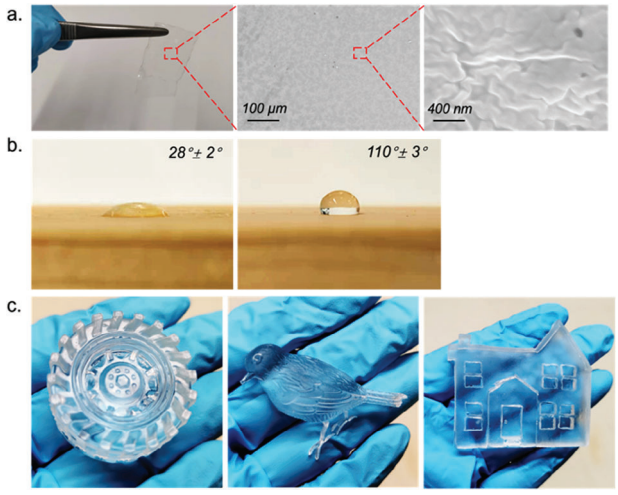

Figure 4. a) Thin films of poly(ethylene glycol) dimethacrylate, b) left: Copolymerized OEGMA/EGDMA as hydrophilic coating on wood surface, right: Copolymerized (tBuA)/EGDMA as hydrophobic coating on wood surface, and c) 3D copolymerized styrene/EGDMA networks: "tyre"-shaped (left), "bird"-shaped (middle), "house"-shaped (right). Reactions were run at ambient temperature in a UV chamber (≈1000 W m^{-2}, sunlight-simulated spectrum). The "bird"-shaped polymer network was synthesized via HPSS-UV-ATRP for 24 h, 100 ppm $CuBr_2$ was added. The ratio of [$CuBr_2$] to [Me_6TREN] was maintained at 1:2. In all the other cases, 18 h HPSS-UV-FRP was conducted at ambient temperature.

eliminates the need for expensive crosslinking agents and alleviates concerns regarding mixing uniformity. HPSS-UV-FRP and HPSS-UV-ATRP have demonstrated to be efficient, versatile, and controlled grafting techniques that are compatible with thin films, coatings, and delicate 3D composites.

The generation of radicals occurs through UV irradiation, through either photodissociation or H-abstraction mechanisms. This process allows for the polymerization of technologically important polymers like methacrylates, acrylates, and styrene, all while operating under mild conditions and without the requirement of externally added initiators. By employing a sufficient amount of $CuBr_2$ (1000 ppm), better control within the system can be achieved by HPSS-UV-ATRP. These unique characteristics offer a wide range of potential applications in photopolymerization.

These collective research endeavors not only advance the knowledge of photopolymerization techniques but also showcase the immense potential of sunlight as an abundant and renewable energy source for polymer synthesis with a broad range of industrial applications.

Supporting Information

Supporting Information is available from the Wiley Online Library or from the author.

Acknowledgements

This work was supported by the ETH Career Seed Award 1–009041. L.H. is supported by funding from the European Research Council (ERC) under the European Unions Horizon 2020 research and innovation programme grant agreement No 801781. L.H. further acknowledges support from the Deutsche Forschungsgemeinschaft (DFG, German Research Foundation) under the Germany's Excellence Strategy EXC 2181/1 – 390900948 (the Heidelberg STRUCTURES Excellence Cluster). The authors thank Prof. Dr. Ingo Burgert (ETH Zürich) for his continuous support.

Conflict of Interest

The authors declare no conflict of interest.

Data Availability Statement

The data that support the findings of this study are available from the corresponding author upon reasonable request.

Keywords

atom transfer radical polymerization, free radical polymerization, high power UV, polymeric materials, thin films

Received: December 28, 2023
Published online:

[1] a) S. Dadashi-Silab, S. Doran, Y. Yagci, *Chem. Rev.* **2016**, *116*, 10212; b) M. Flejszar, P. Chmielarz, M. Giessl, K. Wolski, J. Smenda, S. Zapotoczny, H. Cölfen, *Polymer* **2022**, *242*, 124587.
[2] a) P. Chmielarz, M. Fantin, S. Park, A. A. Isse, A. Gennaro, A. J. D. Magenau, A. Sobkowiak, K. Matyjaszewski, *Prog. Polym. Sci.* **2017**, *69*, 47; b) I. Zaborniak, P. Chmielarz, K. Wolski, G. Grzes, A. A. Isse, A. Gennaro, S. Zapotoczny, A. Sobkowiak, *Macromol. Chem. Phys.* **2019**, *220*, 1900073; c) I. Zaborniak, P. Chmielarz, M. R. Martinez, K. Wolski, Z. Y. Wang, K. Matyjaszewski, *Eur. Polym. J.* **2020**, *126*, 109566.
[3] H. Mohapatra, M. Kleiman, A. P. Esser-Kahn, *Nat. Chem.* **2017**, *9*, 135.
[4] Y. N. Zhou, J. J. Li, Y. Y. Wu, Z. H. Luo, *Chem. Rev.* **2020**, *120*, 2950.
[5] C. Aydogan, G. Yilmaz, A. Shegiwal, D. M. Haddleton, Y. Yagci, *Angew Chem. Int. Ed. Engl.* **2022**, *61*, e202117377.
[6] M. D. Ryan, R. M. Pearson, T. A. French, G. M. Miyake, *Macromolecules* **2017**, *50*, 4616.

[7] a) S. Dadashi-Silab, I. H. Lee, A. Anastasaki, F. Lorandi, B. Narupai, N. D. Dolinski, M. L. Allegrezza, M. Fantin, D. Konkolewicz, C. J. Hawker, K. Matyjaszewski, *Macromolecules* **2020**, *53*, 5280; b) S. Shanmugam, J. T. Xu, C. Boyer, *Macromol. Rapid Commun.* **2017**, *38*, 1700143; c) A. E. Enciso, L. Y. Fu, A. J. Russell, K. Matyjaszewski, *Angew Chem. Int. Ed. Engl.* **2018**, *57*, 933; d) E. R. Ruskowitz, C. A. DeForest, *Nat. Rev. Mater.* **2018**, *3*, 17087.
[8] X. L. Hu, G. Szczepaniak, A. Lewandowska-Andralojc, J. Jeong, B. D. Li, H. Murata, R. G. Yin, A. M. Jazani, S. R. Das, K. Matyjaszewski, *J. Am. Chem. Soc.* **2023**, *145*, 24315.
[9] a) H. L. Wang, H. R. Brown, *Macromol. Rapid Commun.* **2004**, *25*, 1095; b) W. B. Sheng, B. Li, X. L. Wang, B. Dai, B. Yu, X. Jia, F. Zhou, *Chem. Sci.* **2015**, *6*, 2068.
[10] B. Li, B. Yu, F. Zhou, *Macromol. Rapid Commun.* **2014**, *35*, 1287.
[11] K. Sun, H. Chen, Y. J. Zhang, F. Morlet-Savary, B. Graff, P. Xiao, F. Dumur, J. Lalevee, *Eur. Polym. J.* **2021**, *151*, 110410.
[12] C. Hu, P. Bonn, D. E. Demco, C. Bolm, A. Pich, *Angew Chem. Int. Ed. Engl.* **2023**, *62*, e202305783.
[13] K. Mielczarek, M. Labanowska, M. Kurdziel, R. Konefal, H. Benes, S. Bujok, G. Kowalski, S. Bednarz, *Macromol. Rapid Commun.* **2020**, *41*, 1900611.
[14] C. Kutahya, P. Wang, S. J. Li, S. X. Liu, J. Li, Z. J. Chen, B. Strehmel, *Angew Chem. Int. Ed. Engl.* **2020**, *59*, 3166.
[15] a) Y. N. Zhou, J. K. Guo, J. J. Li, Z. H. Luo, *Ind. Eng. Chem. Res.* **2016**, *55*, 10235; b) X. C. Pan, N. Malhotra, S. Dadashi-Silab, K. Matyjaszewski, *Macromol. Rapid Commun.* **2017**, *38*, 1600651.
[16] M. A. Stager, B. Adhikari, A. Raichart, M. D. Krebs, *ACS Macro Lett.* **2023**, *12*, 65.
[17] a) E. Liarou, Y. S. Han, A. M. Sanchez, M. Walker, D. M. Haddleton, *Chem. Sci.* **2020**, *11*, 5257; b) W. Q. Yan, S. Dadashi-Silab, K. Matyjaszewski, N. D. Spencer, E. M. Benetti, *Macromolecules* **2020**, *53*, 2801.
[18] a) J. Lalevée, J. P. Fouassier, *Polym. Chem.* **2011**, *2*, 1107; b) S. Dadashi-Silab, M. A. Tasdelen, B. Kiskan, X. C. Wang, M. Antonietti, Y. Yagci, *Macromol. Chem. Phys.* **2014**, *215*, 675; c) D. Konkolewicz, K. Schröder, J. Buback, S. Bernhard, K. Matyjaszewski, *ACS Macro Lett.* **2012**, *1*, 1219.
[19] a) Y. J. Zhang, Z. Liu, T. Borjigin, B. Graff, F. Morlet-Savary, M. Schmitt, D. Gigmes, F. Dumur, J. Lalevée, *Green Chem.* **2023**, *25*, 6881; b) M. Ciftci, M. A. Tasdelen, Y. Yagci, *Polym. Chem.* **2014**, *5*, 600.
[20] F. Bauer, U. Decker, S. Naumov, C. Riedel, *Prog. Org. Coat.* **2014**, *77*, 1085.
[21] a) M. Panagiotopoulou, S. Beyazit, S. Nestora, K. Haupt, B. T. S. Bui, *Polymer* **2015**, *66*, 43; b) A. Jagtap, A. More, *Polym. Bull.* **2022**, *79*, 8057.
[22] S. Liu, L. Chua, A. A. Shamsabadi, P. Corcoran, A. Patra, M. C. Grady, M. Soroush, A. M. Rappe, *Macromolecules* **2021**, *54*, 7925.
[23] C. R. Becer, R. Hoogenboom, D. Fournier, U. S. Schubert, *Macromol. Rapid Commun.* **2007**, *28*, 1161.
[24] S. C. Ligon, B. Husár, H. Wutzel, R. Holman, R. Liska, *Chem. Rev.* **2014**, *114*, 557.